

THE PUZZLE OF SILICON, TITANIUM, AND MAGNESIUM ANOMALIES IN METEORITIC SILICON CARBIDE GRAINS

ROBERTO GALLINO¹

Istituto di Fisica Generale dell'Università, Via P. Giuria 1, 10125 Torino, Italy

CLAUDIA M. RAITERI AND MAURIZIO BUSO

Osservatorio Astronomico di Torino, Strada Osservatorio 20, 10025 Pino Torinese, Italy

AND

FRANCESCA MATTEUCCI

European Southern Observatory, Karl-Schwarzschild-Strasse 2, D-8046, Garching bei München, Germany

Received 1993 May 10; accepted 1994 January 28

ABSTRACT

An astrophysical interpretation of the silicon, titanium, and magnesium isotope anomalies measured in the mainstream population of single silicon carbide (SiC) grains extracted from carbonaceous meteorites is presented. The condensation site of the grains is envisaged in the cool atmospheres of carbon stars. The Si isotope anomalies show a general linear correlation between $^{29}\text{Si}/^{28}\text{Si}$ and $^{30}\text{Si}/^{28}\text{Si}$, whose slope cannot be explained only by *s*-processing in the He-burning shell and dilution with material of solar composition from the envelope. We suggest a multiple star scenario in which the SiC grains form in stellar envelopes with slightly nonsolar initial Si isotope composition and metallicities from one-half solar to solar. The initial Si abundances are inferred from considerations of galactic chemical evolution, coupling spectroscopic observations of abundances in stars of different metal content with current predictions of stellar nucleosynthesis. The isotopes ^{29}Si and ^{30}Si are assumed to be entirely produced by short-lived massive stars exploding as supernovae, which also contribute $\sim 70\%$ of the solar ^{28}Si abundance, the remaining $\sim 30\%$ coming from long-lived stars, evolving in binary systems, and leading to supernovae of Type Ia. More detailed calculations of the Si isotopes yields from stars of various mass and initial metallicity are, however, required, and a better understanding of how the nucleosynthetic ejecta by supernovae are well homogenized with the interstellar matter. Even the Ti isotope anomalies in SiC grains cannot be explained as only an *s*-process signature. The linear correlation shown by Ti and Si anomalies indicates that a similar approach can be used to interpret the Ti anomalies as a mixture of a pure *s*-component and of a variable nonsolar isotopic composition initially present in the envelope of carbon stars. The question of the large abundance of extinct ^{26}Al in many SiC grains is also considered. We find that the production of ^{26}Al in the H shell of thermally pulsing AGB stars, although followed by substantial consumption by neutron captures during He thermal pulses, can account for the high $^{26}\text{Al}/^{27}\text{Al}$ ratios. The spread of carbon anomalies is interpreted as a consequence of an initial spread of $^{12}\text{C}/^{13}\text{C}$ as observed in M stars and of the subsequent enrichment in ^{12}C of the envelope during thermal pulses. Finally, the nitrogen isotope anomalies are discussed.

Subject headings: circumstellar matter — dust, extinction — meteoroids —
 nuclear reactions, nucleosynthesis, abundances — stars: carbon — stars: evolution

1. INTRODUCTION

Large anomalies in C, Si, N, and noble gases have been found in microsize SiC crystals extracted from carbonaceous meteorites, suggesting their extrasolar origin (Zinner, Tang, & Anders 1987, 1989; Tang & Anders 1988). Heavy noble gases, and other trace elements such as Ba, Nd, and Sm, show the characteristic mark of the *s*-process (Ott et al. 1988; Lewis, Amari, & Anders 1990; Ott & Begemann 1990; Zinner, Amari, & Lewis 1991b; Gallino et al. 1990; Prombo et al. 1993; Gallino, Raiteri, & Busso 1993). In the so-called three-isotope plot different isotopic abundance ratios with respect to a selected isotope assumed as reference correlate linearly, indicating a mixture in variable degree of two components, one pure-*s* (the *G*-component), the other close to solar (the *N*-component).

The SiC grains condense in a reducing environment, when $\text{C}/\text{O} \geq 0.8$ (Larimer & Bartholomay 1979; Lattimer,

Schramm, & Grossman 1978). The most likely astrophysical scenario envisages the extended mass-losing cool atmospheres of carbon stars, which show enhanced abundances of ^{12}C and *s*-process nuclei (see review by Smith & Lambert 1990). In this connection it is important to recall that a broad SiC emission feature at $11.4\ \mu\text{m}$ is observed in the circumstellar envelopes of carbon stars (see discussion in Omont 1993). The feature is actually used as an identifying criterium for carbon stars in the IRAS Catalogue (Chan & Kwok 1990).

Carbon stars are red supergiants of low mass suffering He-shell thermal pulses on the asymptotic giant branch (hereafter TP-AGB). During the recurrent pulses, *s*-processing takes place in the convective He-shell, giving rise to an exponential distribution of neutron exposures. After each pulse, a small amount of newly synthesized products (^{12}C and *s*-nuclei) are mixed to the surface by the downward extension of the envelope convection (the third Dredge-up; see Iben & Renzini 1984).

Although well ascertained on observational grounds, one must say that the stellar evolutionary theory is faced with

¹ Visiting Associate at the Division of Geological and Planetary Sciences, California, Institute of Technology.

difficulties in order to fully account for the third dredge-up mechanism in carbon stars (see Sackmann, & Boothroyd 1991a, b; Vassiliadis & Wood 1993). However, making use of updated mixing length to pressure scale height ratios and of new opacity tables accounting for molecular opacities, recently theoretical models have confirmed the occurrence of these mixing events in stars of masses down to $2.5\text{--}3 M_{\odot}$ (Busso et al. 1993; Chieffi, Limongi, & Straniero 1993).

A more critical problem is to provide a quantitative estimate of the newly synthesized ^{13}C reservoir to be engulfed by each thermal instability. Indeed, ^{13}C is the only efficient neutron source that can operate at the mild He-shell temperature conditions in low-mass TP-AGB stars. This requires a very detailed treatment of the intershell region to mix a few hydrogen atoms from the envelope into the ^{12}C -rich, partially He-burned zone (Iben & Renzini 1984).

Under the hypothesis that meteoritic SiC grains condensed in the circumstellar envelopes of carbon stars, they must carry the memory of two chemical components: one comes from the He shell matter mixed with the envelope after several dredge-up episodes; the second comes from the envelope with modified CNO composition after the first dredge-up, which occurred when the star first became a red giant (Iben 1977).

The major problem with the above picture is to provide a satisfactory interpretation of all isotopic anomalies so far detected, in SiC grains, starting from the most abundant Si and C. While the measured spread of $^{12}\text{C}/^{13}\text{C}$ values can be understood in the light of their carbon star origin (see § 7), the explanation of Si isotope anomalies still stands as a matter of debate. Similar difficulties arise from the analysis of titanium, aluminum, and nitrogen, which are the most abundant trace elements in SiC. Notice that during the He thermal instabilities, the abundance of the light species may either be depleted by α captures (as in the case of ^{13}C , ^{14}N), or slightly affected by neutron captures (as for Si and Ti isotopes). Large enhancements (100–1000 times the initial abundance) are instead achieved by the *s*-only nuclei beyond ^{56}Fe , the exact value depending on the mean neutron exposure (Gallino, Raiteri, & Busso 1993).

1.1. Silicon Anomaly

Let us recall the major experimental results concerning silicon. Zinner et al. (1987) made ion probe analysis of samples of SiC from the Murray CM2 meteorite, finding highly anomalous Si. Subsequently, Tang et al. (1989) and Zinner et al. (1989) reported data on SiC from the Murchison CM2 chondrite, including single grains. The neutron-rich Si isotopes showed excesses with respect to the solar composition ranging up to $\sim 100\%$. The per mil variations are commonly indicated using the “delta” notation: $\delta^i\text{Si} = [(^i\text{Si}/^{28}\text{Si})/(^i\text{Si}/^{28}\text{Si})_{\odot} - 1] \times 1000$.

Amari, Zinner, & Lewis (1991a) presented the first data on the Si compositions in bulk samples of the fine-grained Murchison grain size separates KJA (mass weighted mean diameter $0.38 \mu\text{m}$), KJB ($0.49 \mu\text{m}$), KJC ($0.67 \mu\text{m}$), KJD ($0.81 \mu\text{m}$), KJE ($1.14 \mu\text{m}$), and compared them to isotopic anomalies of single grains of the KJB fraction ($3.02 \mu\text{m}$; Lewis, Amari, & Anders 1994). They found small variations among different size fractions, the bulk of SiC grains of different mean sizes showing $\delta^{29}\text{Si}$ values ranging from 22 to 51 and $\delta^{30}\text{Si}$ values from 29 to 50. A family of “platy” SiC grains was identified by Stone et al. (1991a, b; see also Huss, Hutcheon, & Wasserburg 1993; Huss et al. 1993) in both the Orgueil and the Murchison meteorites.

In the three-isotope plot $\delta^{29}\text{Si}$ correlates linearly versus $\delta^{30}\text{Si}$: the best-fit line does not pass exactly through the point representing the solar composition and has a slope of 1.4. An extensive analysis of single SiC grains has been made by Hoppe et al. (1994), in the study of the coarse grain size separates KJG and KJH ($4.57 \mu\text{m}$). Additional data on KJF ($0.67 \mu\text{m}$) can be found in Hoppe et al. (1993a, b). A number of SiC grains from nine chondritic meteorites (including Murchison, but also unequilibrated ordinary chondrites and enstatite chondrites) were analyzed by Alexander (1993). The three-isotope plot of all existing data on Si confirms the existence of a “mainstream” population, whose $\delta^{29}\text{Si}$ and $\delta^{30}\text{Si}$, ranging up to ~ 200 and 150 , linearly correlate with a slope of ~ 1.3 .

A peculiar feature was discovered by Virag et al. (1992) while determining the Si isotope composition in large single grains of the LS and LU separates ($\sim 5\text{--}20 \mu\text{m}$) from Murchison: the data aggregate into three clusters, presumably a sign of discrete sources. The same clustering is found when the silicon and carbon compositions are considered. While cluster I is made of grains with about normal isotopic composition and could be derived from either contamination or from special reservoirs at reducing conditions in the solar nebula (Larimer & Bartholomay 1979; Stone et al. 1991a; Lodders & Fegley 1993; Alexander 1993), highly anomalous C and Si characterize clusters II and III. In the $\delta^{29}\text{Si}$ versus $\delta^{30}\text{Si}$ plot, these two latter are linked by a best-fit regression line of slope ~ 1.2 , the intracluster data showing a lower slope.

Other minor distinct populations of grains, the very exotic population X consisting of five grains from Murchison KJG and KJH separates (Amari et al. 1992) and three from other chondrites (Alexander 1993), and the population Y (Hoppe et al. 1994), have also been found, both showing light carbon ($^{12}\text{C}/^{13}\text{C} > 89$). As for their Si composition, the X population exhibits large negative $\delta^{29}\text{Si}$ (ranging from -250 to -500) and $\delta^{30}\text{Si}$ (from -400 to -600) values; the Y grains instead show $\delta^{29}\text{Si}$ and $\delta^{30}\text{Si}$ in the range -16 to 24 and 8 to 135 , respectively. A possible new population, called Z, was identified by Alexander (1993) in the Bishunpur (L/LL3.1) and in the Inman meteorites (L/LL3.4), showing $\delta^{29}\text{Si}$ from -70 to -50 , $\delta^{30}\text{Si}$ from -120 to $+180$ and $^{12}\text{C}/^{13}\text{C}$ from 45 to 65 .

The major difficulty with the TP-AGB origin of SiC grains is that the range of ^{29}Si and ^{30}Si excesses one expects from the *s*-process in the He shell would plot quite below the measured correlation line, with a predicted slope of ~ 0.5 (Gallino et al. 1990; Obradovic et al. 1991). Furthermore, the theoretical $\delta^{29}\text{Si}$ and $\delta^{30}\text{Si}$ values would cover a much smaller spread, owing to the low *s*-process imprint on Si.

1.2. Titanium Anomaly

Titanium is likely to have condensed as titanium carbide at slightly higher temperatures than SiC. Minute crystals of TiC have been detected inside a large SiC grain (Bernatowicz et al. 1992), as well as inside one graphite grain (Bernatowicz et al. 1991).

Ireland, Zinner, & Amari (1991a) analyzed 14 large grains ($8\text{--}23 \mu\text{m}$) of the LU series. They determined a highly anomalous Ti composition for nine of them. Moreover, a good correlation between Si and Ti was found, the grains with the greatest excesses of ^{50}Ti also having the highest excesses of ^{29}Si . All Ti isotopes show per mil excesses (with ^{48}Ti as the reference isotope). This trend was recognized to be only in qualitative agreement with the *s*-processing in the He shell of TP-AGB stars, from which lower $\delta^{46}\text{Ti}$ excesses would ensue.

Amari, Zinner, & Lewis (1991b) examined fine-grained aggregates (0.1–0.2 μm) of the KJB fraction. These grains show lower values of $\delta^{46}\text{Ti}$, $\delta^{47}\text{Ti}$, and $\delta^{49}\text{Ti}$ than the grains of the LU separate. As reported in the accompanying paper by Hoppe et al. (1994), a sample of 21 single grains (3–5 μm) from KJB were analyzed for Ti. Most of them show excesses of all Ti isotopes, with a large scatter in the three-isotope plots. However, a clear correlation is found between $\delta^{29}\text{Si}$ and $\delta^{46}\text{Ti}$, with a mean slope ~ 1 . The correlation versus $\delta^{29}\text{Si}$ is more difficult to trace for the other Ti isotopes, or even not distinguishable, as for ^{50}Ti . In spite of the paucity of data, an interesting feature was recognized by Hoppe et al. (1993): the data clusters of Si and C anomalies identified by Virag et al. (1992) are also present when considering the Ti isotopic composition of these grains.

1.3. Magnesium Anomaly

The ^{26}Mg excess measured in many SiC grains provides evidence of the “in situ” decay of extinct ^{26}Al .

An analysis of four SiC separates (HM, HN, KJG, and LS + LU) from Murchison has been made by Zinner et al. (1991a). As for KJG and LS + LU fractions, it was possible to measure the ^{26}Mg excess in single grains: in KJG a clear ^{26}Mg excess was revealed in about half of the grains, the $^{26}\text{Al}/^{27}\text{Al}$ ratio ranging from 10^{-4} to 0.2; in LS + LU only two grains show a definite ^{26}Mg excess corresponding to a few 10^{-3} in the $^{26}\text{Al}/^{27}\text{Al}$ ratio. In the companion paper by Hoppe et al. (1994), more data on KJG and grains from the KJB separate are analyzed for Mg and Al, confirming and extending the previous results. The $^{26}\text{Mg}/^{24}\text{Mg}$ excesses they found are enormous, up to 7000 times the solar value, while no excess is found in the $^{25}\text{Mg}/^{24}\text{Mg}$ ratio inside the error bars. The ^{26}Al signature carried by SiC grains must be interpreted as a fossil “cosmic chemical memory” (Clayton 1977), already extinct when the grains were trapped in the early solar system. Instead, live ^{26}Al was ascertained in the early solar system, at a canonical value of $^{26}\text{Al}/^{27}\text{Al} = 5 \times 10^{-5}$ in Ca-, Al-rich Inclusions (CAI) of primitive meteorites (Lee, Papanastassiou, & Wasserburg 1977; Wasserburg 1985). The unstable ^{26}Al is a product of hot shell H-burning, which is easily consumed by neutron captures during the He thermal instabilities. However, the occurrence of the third dredge-up after each pulse also mixes with the envelope ashes of the temporary inactivated H shell, bringing to the surface ^{26}Al that can pass to the interstellar medium. To this regard, it has recently been suggested that a single TP-AGB star most likely polluted the early solar nebula with ^{26}Al , together with other short-lived radioactive nuclei (Wasserburg et al. 1994).

In this paper we suggest a possible way to interpret the Si, Ti, and Mg anomalies in the framework of a multiple TP-AGB star origin of SiC grains, in which they carry not only the signature of the *s*-process, but also that of a slightly nonsolar Si and Ti isotope composition, as a consequence of the chemical evolution of the Galaxy. In § 2 the Si composition due to *s*-processing in TP-AGB stars of low mass is presented: it is inferred from new nucleosynthesis calculations with updated neutron capture cross sections. Then, in § 3, the production of the Si isotopes by supernovae models is analyzed, and the trend of the Si isotopic abundances with metallicity is tested with a model for the chemical evolution of the Galaxy. The consequences of the galactic chemical evolution for the Si isotope anomalies in SiC grains are derived in § 4, where a whole set of stellar results is given and compared with the

meteoritic data. The same approach is applied in § 5 to the interpretation of the Ti isotope anomalies in SiC grains. The large abundance of extinct ^{26}Al measured in a number of SiC grains is analyzed in § 6, and the problem of the large and uncorrelated carbon and nitrogen isotope anomalies is discussed in § 7. The main conclusions of this paper are given in § 8.

2. Si COMPOSITION FROM THE *s*-PROCESS

The stellar modeling we adopted to follow the *s*-processing during the TP-AGB phase and the *s*-enrichment of the envelope has been described in previous papers (see, e.g., Käppeler et al. 1990; Busso et al. 1992; Gallino, Raiteri, & Busso 1993). We recall here that the neutron source in the He thermal pulse mainly derives from the reaction $^{13}\text{C}(\alpha, n)^{16}\text{O}$, which releases neutrons when the bottom temperature of the He shell is close to 1.5×10^8 K. We assume that the amount of ^{13}C ingested during each pulse is $9 \times 10^{-6} M_{\odot}$ and that it does not depend on the metal content of the star. The maximum mean neutron density averaged over the thermal pulse region is $\sim 4 \times 10^8 \text{ cm}^{-3}$. A second minor burst of neutrons is released by α -captures on ^{22}Ne at higher temperature (3.0×10^8 K) near the end of the instability, the peak of the mean neutron density reaching $\sim 10^9 \text{ cm}^{-3}$.

As recalled in § 1, neutrons are captured not only by heavy seeds of the ^{56}Fe peak and beyond, but also by the lighter nuclides present in the environment, on the base of their cross sections and relative concentrations. The abundance changes of these light species are, however, rather small when compared with the mean production factors achieved by the *s*-only nuclei beyond ^{56}Fe . This is so also for ^{25}Mg , that is currently considered as the most important “neutron poison.” Concerning Si isotopes, in TP-AGB stars of initial solar metallicity the *s*-process occurring during thermal pulses slightly decreases the initial ^{28}Si abundance, by 6%, while increasing ^{29}Si by 40% and ^{30}Si by a factor 1.8, corresponding to $\delta^{29}\text{Si} = 430$ and $\delta^{30}\text{Si} = 910$.

These results have been obtained taking into account of the important feedback reaction affecting the ^{30}Si production: $^{33}\text{S}(n, \alpha)^{30}\text{Si}$. Its Maxwellian-averaged cross section is 217 ± 20 mbarn at 30 keV (Wagemans, D’hondt, & Brissot 1993), i.e., ~ 40 times higher than the neutron capture cross section of ^{30}Si . As for the radiative neutron captures, Beer, Voss, & Winters (1992, hereafter BVW92) have recently published a new compilation, where the temperature-dependence of cross sections for most of the isotopes involved in the *s*-process is included. In many cases, large deviations from the $1/v$ law are found. Since the release of neutrons by the ^{13}C source in a thermal pulse occurs when the thermal energy at the bottom is $\simeq 12$ keV, i.e., far from the 30 keV at which cross sections are usually given, such deviations can have significant effects. Apart from ^{56}Fe , this is particularly evident for all the Si isotopes, as already stressed by Bao & Käppeler (1987).

The 30 keV Maxwellian average cross section of ^{28}Si quoted by BVW92 is lower by 40% than the one given by Bao & Käppeler (1987). However, a theoretical reevaluation (Beer 1992) confirms the older estimate, so that we took the temperature dependence from BVW92, normalizing it to the 30 keV value of Bao & Käppeler (1987).

In Table 1 the Si neutron capture cross sections adopted in this paper are shown both during the operation of the ^{13}C neutron source ($kT = 12$ keV) and of the ^{22}Ne source ($kT = 26$

TABLE 1
NEUTRON CAPTURE CROSS SECTIONS ADOPTED IN OUR NETWORK^a

Isotope	$\bar{\sigma}(kT = 12 \text{ keV})^b$	$\bar{\sigma}(kT = 26 \text{ keV})^b$	$\bar{\sigma}(kT = 30 \text{ keV})^c$
²⁸ Si.....	0.76	2.36	2.9 ± 0.3^d
²⁹ Si.....	8.79	8.87	7.9 ± 0.9
³⁰ Si.....	20.2	9.12	6.4 ± 0.6
⁴⁶ Ti.....	20.4	24.7	26.5 ± 3.2
⁴⁷ Ti.....	82.4	70.5	64.8 ± 7.7
⁴⁸ Ti.....	36.1	34.2	30.8 ± 5.1
⁴⁹ Ti.....	22.4	22.8	22.1 ± 2.1
⁵⁰ Ti.....	1.37	3.18	4.0 ± 0.5

^a In mbarns.

^b All cross sections are given as $\bar{\sigma} = \langle \sigma_{n,\gamma}(kT) \rangle \times [kT/(30 \text{ keV})]^{1/2}$ to underline deviations from the classical $1/v$ law. From this paper.

^c From Beer, Voss, & Winters 1992.

^d From Bao & Käppeler 1987.

keV). In order to emphasize the deviations from the $1/v$ law, they are presented as $\langle \sigma_{n,\gamma}(kT) \rangle \times [kT/(30 \text{ keV})]^{1/2}$; the values at 30 keV recommended by BVW92 are included in the last column of the table for comparison.

To follow the process of mixing of He shell matter with the envelopes we adopted a simplified scheme, based on the Chieffi et al. (1993) models: the penetration of the envelope convection after each pulse is assumed to be roughly of $10^{-3} M_{\odot}$. On the whole, to obtain a C-star ($C/O \approx 1$) one has to mix one part of He-shell matter for any 40–50 parts of the original envelope, the precise dilution factor depending also on mass loss (see Busso et al. 1992, 1994 for details). The predicted $\delta^{29}\text{Si}$ and $\delta^{30}\text{Si}$ excesses in the envelope of carbon stars reach values up to ~ 10 and ~ 20 , respectively, when assuming in the envelope an initial solar Si composition. Moreover, the predicted slope of the $\delta^{29}\text{Si}$ correlation line is ~ 0.5 , distinct from the observed one.

About the same results are found for disk stars of metallicity lower than solar, both in the He shell (see Table 2) and in the envelope, assuming the initial Si isotope composition to scale linearly with metallicity. Similar conclusions were obtained previously (Gallino et al. 1990; Obradovic et al. 1991), using the Bao & Käppeler (1987) prescriptions for neutron capture cross sections. The consequences on all the Si isotopes of the refined radiative neutron capture cross sections are hidden by the much higher feedback effect on the ³⁰Si abundance due to the ³³S(n, α)³⁰Si reaction. However, a better evaluation of the

temperature dependence of all Si isotopes at thermal energies lower than 30 keV is highly required for a better understanding of the Si anomalies. At the present state of the art, the s-process nucleosynthesis alone can explain neither the large spread of data measured in SiC nor the unity slope in the Si three-isotope plot.

3. GALACTIC EVOLUTION OF SILICON ISOTOPES

An attempt to explain the Si isotope anomalies in SiC grains in terms of nucleosynthetic processes occurring inside a TP-AGB star, but with an ad hoc enhancement of the He shell temperature has been done by Brown & Clayton (1992, 1993; see discussion in § 4.1).

We follow here a different point of view (first discussed in Gallino, Raiteri, & Busso 1992), where we consider a combination of s-processing and of a nonsolar isotopic Si initial composition in stellar envelopes due to the chemical evolution of the Galaxy.

The idea that the chemical evolution of the Galaxy could be crucial for interpreting the Si anomalies in SiC grains was anticipated by Clayton (1988), under the hypothesis that refractory dusts condense in the winds of stars of all types at the epoch of solar system formation with an isotopic composition averaged on the ejecta of a generation of stars, a linear formation rate, and instantaneous recycling approximation. Moreover, ^{29,30}Si were considered to scale as Z^2 and ²⁸Si to scale as Z .

Assuming no infall of metal-free gas from the galactic halo, a large and fixed value for $\delta^{29,30}\text{Si}$ of 560 was predicted in all dust grains. While the introduction of a given amount of metal-free infall matter on the Galactic disk lowers the above δ excesses, thus better approaching the observed anomalies in SiC, the fact that SiC grains condense only in carbon-rich long-lived stars makes necessary to release the instantaneous recycling approximation.

Anyhow, the possible imprint of the chemical evolution of the Galaxy in stardust grains is worthwhile for a deeper scrutiny. This possibility has been recently taken again by Alexander (1993) for both Si and Ti. The author favors a multistar origin for the SiC grains and estimates 10–100 TP-AGB stars salting the protosolar nebula.

Before affording the problem of the interpretation of Si anomalies in SiC grains, we must discuss the observational and

TABLE 2
SI ISOTOPE COMPOSITIONS IN THE HE SHELL OF TP-AGB STARS AND INITIAL COMPOSITIONS

ISOTOPE	[Fe/H], τ_0 (mbarn ⁻¹)						
	-0.52, 0.277	-0.35, 0.215	-0.22, 0.179	-0.12, 0.154	-0.05, 0.137	+0.00, 0.128	+0.10, 0.109
Production Factors ($X_i^{\text{fin}}/X_i^{\text{ini}}$)							
²⁸ Si.....	0.879	0.905	0.921	0.932	0.940	0.944	0.957
²⁹ Si.....	1.145	1.223	1.273	1.309	1.335	1.349	1.321
³⁰ Si.....	1.641	1.714	1.756	1.782	1.798	1.806	1.751
δ -Values ($\delta^i\text{Si}$)							
²⁹ Si.....	303	351	382	405	420	429	380
³⁰ Si.....	867	894	907	912	913	913	830
Initial Compositions (X_i^{ini})							
²⁸ Si.....	2.80 (-4)	3.73 (-4)	4.54 (-4)	5.34 (-4)	6.11 (-4)	6.53 (-4)	7.59 (-4)
²⁹ Si.....	1.87 (-5)	2.31 (-5)	2.65 (-5)	2.96 (-5)	3.27 (-5)	3.43 (-5)	3.81 (-5)
³⁰ Si.....	1.28 (-5)	1.59 (-5)	1.82 (-5)	2.03 (-5)	2.24 (-5)	2.35 (-5)	2.61 (-5)

theoretical pieces of information that allow us to speculate about the isotopic Si trend along the history of the Galaxy.

High-resolution spectroscopy of halo and disk stars shows that the so-called α -rich elements (O, Mg, Si, S, Ca, and Ti) are enhanced with respect to iron for lower than solar metallicities (see the review papers by Lambert 1989; Ryan, Norris, & Bessell 1991; Edvardsson et al. 1993). According to the usual notation, the metallicity is expressed as $[\text{Fe}/\text{H}]$, where $[\text{Fe}/\text{H}] = \log(\text{Fe}/\text{H})_* - \log(\text{Fe}/\text{H})_\odot$. The exact amount of this enhancement is uncertain, since the data show a scatter of the order of ± 0.2 dex. In any case, for halo stars (the most metal poor stars, with $[\text{Fe}/\text{H}] \leq -1$), it is roughly constant, while in the disk ($[\text{Fe}/\text{H}] > -1$) one can approximate the data by a linear decrease: $[\text{N}_\alpha/\text{Fe}] = -a[\text{Fe}/\text{H}]$, the constant a depending on the element considered. The observed trend is interpreted as the result of nuclear processes taking place in stars with different evolutionary timescales: the behavior of the α -rich elements in the halo phase, that lasted for less than 10^9 yr, must be explained in terms of production in short-lived massive stars exploding as Type II supernovae (SNe). On the other hand, also long-lived low-mass stars in addition to massive stars contribute to the chemical enrichment of the disk. It is worth cautioning that $[\text{Fe}/\text{H}]$ can only approximately be used as an indicator of age since, as stressed by Edvardsson et al. (1993), there is a significant spread in the metallicities of stars formed at a given time in the disk.

About one-third of the iron content in the solar system is currently ascribable to Type II SNe, which, however, fully account for the solar oxygen abundance. The remaining $\simeq \frac{2}{3}$ of solar Fe is contributed by Type Ia SNe, which explode on longer timescales and do not produce oxygen (Matteucci & Greggio 1986; Nomoto et al. 1990). We must notice that there is a big uncertainty concerning the amount of iron massive stars can produce.

Observations mainly give us elemental information, while we would like to know the time evolution of every single isotope. In trying to infer isotopic trends, only theoretical results coming from nucleosynthesis calculations are available. Unfortunately, such calculations are affected by a number of uncertainties, related to the choice of some basic nuclear parameters [e.g., the $^{12}\text{C}(\alpha, \gamma)^{16}\text{O}$ reaction rate] and to the difficulty of modeling internal mixing (time-dependent convection, semiconvection, overshooting) and stellar explosion. Moreover, the outgoing supernova burst is artificially ignited, and the cutoff mass separating the stellar remnant from the ejecta has to be calibrated against observations.

Theoretical predictions for the isotopic composition of ejecta of a typical Type II SNe have been derived by Thielemann, Hashimoto, & Nomoto (1990), starting from a stellar model with a helium core mass $M_\alpha = 6 M_\odot$ (the supposed progenitor of SN 1987A). They found that production of ^{29}Si and ^{30}Si is a factor of 2 higher than that of ^{28}Si . Recent results by Hashimoto et al. (1993) obtained by averaging the chemical yields of stars with different masses confirm that more $^{29,30}\text{Si}$ than ^{28}Si is produced in Type II supernovae. A greater production of ^{29}Si and ^{30}Si with respect to ^{28}Si was also found by Woosley (1986), although this feature is no longer evident in more recent calculations (Weaver & Woosley 1993).

A study of the composition of the ejecta of a typical carbon deflagration Type Ia supernova with a solar composition by Thielemann, Nomoto, & Yokoi (1986) reveals that both ^{29}Si and ^{30}Si are underproduced in comparison to ^{28}Si . Recent low-metallicity calculations make this feature even more clear.

Essentially only ^{28}Si can be contributed by Type Ia SNe, up to $\sim 30\%$ of its solar abundance. This is in agreement with early time spectra of Type Ia SNe (Branch et al. 1985). Substantial contributions to ^{28}Si also come out of delayed detonation models by Khoklov (1991; his model 1) and from the detonation models by Shigeyama et al. (1992). These results might provide a clue for the interpretation of the observations: in the halo Si (that is ^{28}Si) shows a lower abundance than oxygen because, while all the solar O is contributed by Type II supernovae, only $\simeq 70\%$ of ^{28}Si can be ascribed to that source (Nomoto et al. 1990). In the disk, this would imply an enhancement of $[\text{Si}/\text{Fe}]$, with a rough correlation $[\text{Si}/\text{Fe}] = -0.3 [\text{Fe}/\text{H}]$, as can also be inferred by the observational trend (Edvardsson et al. 1993).

One must recall that all the above supernova calculations have been performed starting with an initial solar metallicity. An important point is to know whether ^{29}Si and ^{30}Si have a primary or a secondary origin; that is, if they are synthesized inside massive stars starting from H and He or if their production needs ^{22}Ne as seed and is thus metal dependent. The production of the Si isotopes in two $25 M_\odot$ Type II SNe of solar and 0 metallicity was calculated by Timmes, Woosley, & Weaver (1993; see also Woosley & Weaver 1982). The two isotopes $^{29,30}\text{Si}$ are synthesized partly during the He- and C-burning phases through neutron captures activated by the $^{22}\text{Ne}(\alpha, n)^{25}\text{Mg}$ reaction, and mostly during hydrostatic (convective shell) and explosive Ne burning (Woosley 1986; Woosley & Weaver 1980). During hydrostatic Ne burning, their production occurs through the reactions chains (Thielemann & Arnett 1985): $^{23}\text{Na}(\alpha, p)^{26}\text{Mg}(\alpha, n)^{29}\text{Si}$; $^{28}\text{Si}(n, \gamma)^{29}\text{Si}(n, \gamma)^{30}\text{Si}$; $^{24}\text{Mg}(\alpha, p)^{27}\text{Al}(\alpha, p)^{30}\text{Si}$.

In the above reaction chains the starting nuclei are primary species, produced in the star from initial H and He. Since ^{29}Si and ^{30}Si are neutron-rich isotopes, their production requires a neutron excess $\eta = \sum_i (N_i - Z_i) Y_i$, where N_i , Z_i , and Y_i are the number of neutrons, the number of protons and the number density of the species i , respectively. At the beginning of He burning the reaction chain $^{14}\text{N}(\alpha, \gamma)^{18}\text{F}(\beta^+)^{18}\text{O}$ creates a neutron excess, which is metal dependent, since ^{14}N was produced by H burning starting from the initial CNO nuclei. But in the later phases η is substantially increased by weak interactions, the inner regions of stars with different metallicities achieving very close values of the neutron excess (Woosley & Weaver 1982; see, in particular, their Fig. 3). The effect is even more evident during explosive conditions, on which most of the final Si isotope abundances in the ejecta depend.

The trend of the Si abundances with metallicity thus depends on the relative importance of the stellar zones in which they are produced.

In the following we will make an explorative test under the assumption that ^{29}Si and ^{30}Si are synthesized by massive stars in a primary way. This implies in particular that they mimic the $[\text{O}/\text{Fe}]$ behavior versus $[\text{Fe}/\text{H}]$. We have inserted the theoretical yields into the program of galactic chemical evolution developed by Matteucci & François (1989). The Si yields from Type II SNe of different masses were taken from Hashimoto et al. (1993), and those from Type Ia SNe from Thielemann et al. (1986). The observed trend of ^{28}Si with metallicity appears to be satisfactorily reproduced (see Fig. 1), as well as the solar abundances of the three Si isotopes. From the above discussion, it is clear that the trend of the isotopic Si abundances with metallicity in the interstellar medium appears to be a sensitive function of the role played by stars of different

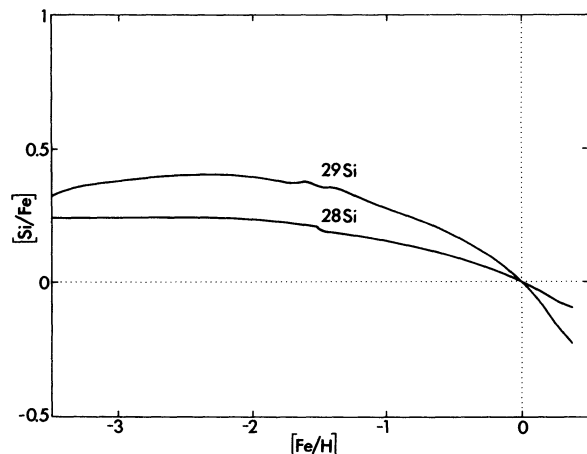


FIG. 1.—The behavior of $[^{28}\text{Si}/\text{Fe}]$ and $[^{29}\text{Si}/\text{Fe}]$ vs. $[\text{Fe}/\text{H}]$ as predicted by the galactic chemical evolution model adopted in this paper.

masses in producing the three isotopes. The situation concerning theoretical predictions is not completely settled, however, since large uncertainties still affect stellar yields from stars of different masses and metallicities. For example, in the galactic halo the behavior of ^{29}Si and ^{30}Si sketched in Figure 1 might not represent the real trend. However, at least for stars of disk metallicity, that are considered as the most likely progenitors of the SiC grains trapped in meteorites, the neutron-rich Si isotopes might be slightly enhanced with respect to ^{28}Si .

In the following we shall examine the influence on SiC grains of a varying Si isotope composition, under the assumption that in the disk $[^{28}\text{Si}/\text{Fe}] = -0.3 [\text{Fe}/\text{H}]$, while $[^{29,30}\text{Si}/\text{Fe}] = -0.5 [\text{Fe}/\text{H}]$. This does not pretend to match the real galactic trend of the Si isotopes, but is a reasonable way to start accounting for a differential behavior with galactic metallicity of the neutron-rich silicon isotopes with respect to ^{28}Si . In this way the Si anomaly carried by SiC grains has a double origin, being ascribable partly to the small s -process signature of the He-shell matter mixed with the envelope during the TP-AGB phase, but chiefly to the original nonsolar Si composition in the envelope. Since a typical dilution factor of ~ 50 parts of original envelope to one part of He-shell matter gives account of the observed chemical composition of carbon stars, a small anomaly in the N -component would easily take the major role. Local chemical inhomogeneities in the evolution of the Galaxy (see, e.g., Maline et al. 1993) could mimic the same effect described above; for example, the formation of low-mass stars inside molecular clouds polluted by supernova ejecta of short-lived massive stars.

4. SILICON ANOMALIES IN SiC GRAINS

Once we have inferred a possible trend for the galactic evolution of the Si isotope composition, we can follow its concentration in the envelope of carbon stars. It varies as a function of both the initial metallicity and the progressive mixing of s -process matter through the various third dredge-up episodes.

Figure 2 shows the results in the three-isotope diagram $\delta^{29}\text{Si}$ versus $\delta^{30}\text{Si}$: they have been obtained at the last pulse before the star leaves the AGB phase. Different symbols are used to indicate the envelope composition when varying the initial metallicity from $[\text{Fe}/\text{H}] \sim -0.5$ to $+0.1$. For a given metallicity, a spread of values along a ≈ 0.5 slope line is found by considering a set of AGB stars of slightly different initial mass:

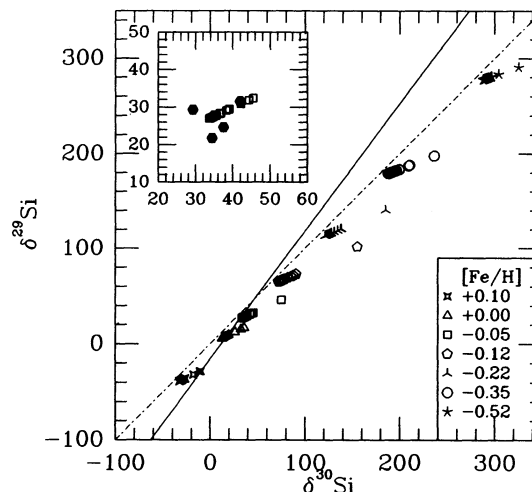


FIG. 2.—Three-isotope plot for Si, showing the results of our calculations in TP-AGB stars. Each sequence of data corresponds to stellar models of given metallicity and masses ranging from 1.5 to $1.7 M_{\odot}$. In the inset the black points representing the bulk compositions of separates KJA-KJE are superposed to the stellar predictions for the case $[\text{Fe}/\text{H}] = -0.05$.

in the figure, 20 stars ranging between 1.5 and $1.7 M_{\odot}$ have been considered, all achieving $\text{C}/\text{O} \geq 1$ in the remaining envelope at the last pulse. The composition at that moment depends on the final dilution of the He-processed matter with the envelope: the more massive the star is, the greater the envelope but also the larger is the number of pulses and dredge-up mixing episodes it experiences. As discussed in Gallino et al. (1993) for the Ba anomalies in SiC grains, about the same spread is obtained when the mass range is extended from 1 to $3 M_{\odot}$. When only a very thin envelope is left at the last pulse, an s -process enriched matter will result, with the possibility of a few SiC grains to show much higher Si excesses. We must notice that similar sequences of data as shown in Figure 2 can be also obtained for the envelope composition of single stars in the more advanced pulses, once $\text{C}/\text{O} \sim 1$ is achieved. However, the condensation of larger SiC grains is favored for higher mass-loss rates and circumstellar densities (Virag et al. 1992), which are more easily obtained at the end of the TP-AGB phase, when the so-called *superwind* phenomenon is likely to occur.

In Figure 2, the solid line represents the Hoppe et al. (1993) best-fit line: $\delta^{29}\text{Si} = 1.34 \times \delta^{30}\text{Si} - 15.7$; it can be seen that the predicted values are close by matching this line. A comparison with the meteoritic data shows that the whole observed range is covered by stellar models within a small range of metallicities $-0.2 \leq [\text{Fe}/\text{H}] \leq +0.2$. The inset figure shows the bulk compositions of the separates KJA to KJE (black points) determined by Amari et al. (1991a); they nicely overlap the sequence of points corresponding to a metallicity $[\text{Fe}/\text{H}] = -0.05$.

The data from cluster II of Virag et al. (1992), have $\delta^{29}\text{Si} = 30$ – 50 , $\delta^{30}\text{Si} = 30$ – 65 , and a slope of ~ 0.5 . They could be nicely interpreted as deriving from a single TP-AGB star of initial metallicity slightly less than solar, the spread of data being the consequence of the s -processing in the last thermal pulses. Analogously, the population Y, laying on a line with a slope ~ 0.5 , can be explained in the framework of TP-AGB nucleosynthesis in single star of about solar metallicity. In our simplified picture, negative $\delta^{29}\text{Si}$ and $\delta^{30}\text{Si}$ values

would characterize the composition of stars with metallicity slightly higher than solar. Indeed, in the framework of the above assumptions, the interstellar medium is progressively enriched in ^{28}Si by the low-mass binary stars exploding as SNe of Type Ia.

The data shown in Figure 2 for $[\text{Fe}/\text{H}] = +0.1$ cover the lower limit of the measured mainstream Si data. The minor population Z may be interpreted in the same context of the grains Y; they indeed show a large spread of $\delta^{30}\text{Si}$, but somewhat more negative $\delta^{29}\text{Si}$ values. However, the statistic of the grains belonging to these minor populations should be improved before drawing any definite conclusion.

We will not consider the subclass of grains X, which exhibit highly negative $\delta^{29,30}\text{Si}$ values, heavy nitrogen and carbon, and extremely high $^{26}\text{Al}/^{27}\text{Al}$ ratios, up to 0.6. As discussed in Hoppe et al. (1993), these grains cannot be originated in carbon stars, and very young supernovae remnants appear the most likely site for their condensation, provided a partial mixing of different shells during the explosion may preserve the necessary high C/O conditions for their formation (Amari et al. 1992).

Figure 3 shows the predicted $\delta^{29}\text{Si}$ values as a function of the $^{12}\text{C}/^{13}\text{C}$ ratio for two different choices of this quantity at the beginning of the AGB phase: for each metal content, the series of data on the left refers to $(^{12}\text{C}/^{13}\text{C})_{\text{ini}} = 8$, while that on the right to 30. In this way, the observational range is covered (see discussion in § 7).

The observed lack of correlation between the Si and C anomalies in SiC grains is easily understood in our scenario: the $^{12}\text{C}/^{13}\text{C}$ ratio is the consequence of internal nucleosynthesis and of the spread of $(^{12}\text{C}/^{13}\text{C})_{\text{ini}}$ resulting after the first dredge-up (and extramixing) in stars of different masses, while the Si excess mainly derives from the differential production of Si isotopes along the chemical evolution of the Galaxy.

4.1. Alternative Astrophysical Sources

A possibility to explain the Si isotope anomalies in SiC grains has been advanced by Brown & Clayton (1992, 1993).

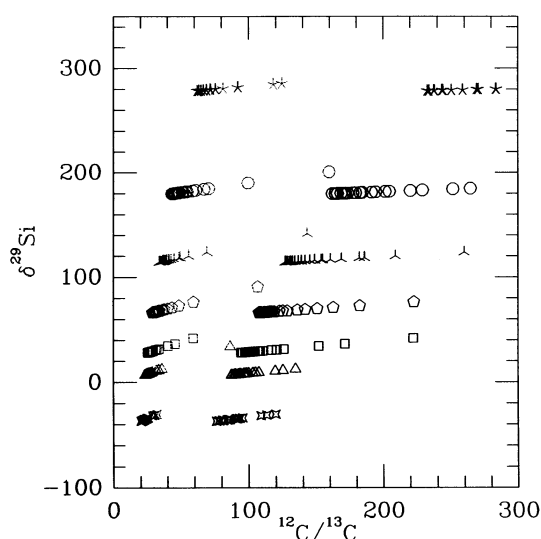


FIG. 3.—The predicted variation of $\delta^{29}\text{Si}$ as a function of the $^{12}\text{C}/^{13}\text{C}$ ratio in stars of various metallicities (see Fig. 2) and masses ranging from 1.5 to 1.7 M_{\odot} . Two different assumptions for the initial $^{12}\text{C}/^{13}\text{C}$ ratio on the AGB are made: 8 (dotted symbols on the left) and 30, to cover the observational range.

They investigated Mg burning by α -capture in the He shell of TP-AGB stars of intermediate mass (6–9 M_{\odot}), in which the peak temperature of the pulse is assumed to be $\sim 20\%$ higher compared to what is currently obtained in stellar evolutionary models. If the temperature is high enough, first ^{24}Mg burns into ^{28}Si by α -captures and ^{25}Mg into ^{29}Si ; then ^{26}Mg burns into ^{30}Si . As a final result, the authors could explain the slope of the correlation line in the Si three-isotope plot of Stone et al. (1991b) by suggesting mixing of the envelope with Mg-processed material in a single AGB star. However, since Mg burning does not affect the Ti isotopes, the correlation between ^{29}Si and ^{46}Ti is left unexplained. Moreover, they predict too high a $^{26}\text{Al}/^{27}\text{Al}$ ratio, the ^{26}Al being produced by hot bottom burning at the base of the convective envelope, where the temperature reaches about $T_6 = 90$. The mechanism would also be responsible for the Ne-E feature shown by the SiC grains through the production of radioactive ^{22}Na (Brown & Clayton 1993). But this origin for ^{22}Ne cannot explain the correlation with ^{4}He which is observed in the SiC grains. Furthermore, the operation of hot bottom burning implies a low $^{12}\text{C}/^{13}\text{C}$ ratio in the envelope, close to the CNO equilibrium value, and a very high $^{14}\text{N}/^{15}\text{N}$ ratio. This is not in agreement with the bulk of the SiC grains. Moreover, proton captures at the bottom of the convective envelope would strongly affect Mg isotopes, with a large reduction of the abundance of ^{24}Mg with respect to ^{25}Mg . Finally, the consumption of ^{22}Ne , ^{25}Mg , and ^{26}Mg by α reactions in the He shell would give rise to a very high average neutron density with a large s -signature in the Kr and in Ba isotopes, involving a strong departure from what is observed in SiC (Lewis et al. 1990; Gallino et al. 1990; Gallino et al. 1993). While it cannot be excluded that improved stellar models in the future will find higher temperatures in the He shell of the most massive TP-AGB stars, making Mg burning possible, the above interpretation will suffer from major difficulties in accounting for the global features observed in SiC grains.

Another scenario for the formation of the SiC grains deals with Wolf Rayet stars, which are considered as very massive stars ($M \geq 40 M_{\odot}$) undergoing strong mass loss. In these stars the original envelope is being peeled off, uncovering first H-processed matter (Of and WN phases) and then He-processed zones (WC and WO phases). Evidence of dust condensation around W-R stars has been found for a few of them (see, e.g., Williams et al. 1992). The point is to see if the conditions to form SiC grains with the observed compositions are met. Prantzos et al. (1986) have calculated abundances in the ejecta of W-R stars in the mass range 50–100 M_{\odot} (see their Table 2). From their data one can infer that when the C/O ratio is favorable for condensation of SiC, the various constraints coming from the measured isotopic ratios are not satisfied. In particular, extremely high $^{12}\text{C}/^{13}\text{C}$ and $^{25}\text{Mg}/^{24}\text{Mg}$ ratios would result, together with a very low N concentration, and too high $\delta^{29}\text{Si}$ and $\delta^{30}\text{Si}$ linearly correlating on a line of slope 0.5.

Finally, we can examine what happens in Type II SNe in the region where $\text{C}/\text{O} \geq 1$. Taking a 25 M_{\odot} star as representative, we find that this requirement is satisfied both in the He shell and in the outer zone of the C-O core, which experienced partial He burning because of the shrinkage of the convective core. In the first zone, the Si isotope composition is solar, while in the second layer a marginal s -process could occur, with neutron exposures in the range $\tau = 0.004\text{--}0.02 \text{ mbarn}^{-1}$. Using the calculations of Raiteri et al. (1993) we derive

$\delta^{29}\text{Si} = 226$ to 661 and $\delta^{30}\text{Si} = 214$ to 807 in this second zone. However, even in this zone ^{13}C has already been fully consumed by α -captures, not fulfilling the observed $^{12}\text{C}/^{13}\text{C}$ ratios.

5. TITANIUM ANOMALIES

In this section we shall try to give an interpretation of the Ti isotope anomalies observed in SiC grains. We will follow the same procedure we used for Si; however, the case of Ti is more complex. First of all, the neutron capture cross sections of the Ti isotopes are known less precisely than those of the Si isotopes: the uncertainty at 30 keV is of the order of 10% – 17% (see Table 1). Moreover, a strong temperature-dependence characterize the $\langle\sigma_{n,\gamma}\rangle$ of the neutron-magic ^{50}Ti , its theoretical extrapolation to 12 keV being lower than the value extrapolated from the $1/v$ law by nearly a factor of 4 . Large departures from the $1/v$ law are also predicted for the cross sections of ^{46}Ti and ^{47}Ti .

By adopting the cross sections and the temperature dependences given by BVW92 (see Table 1), we calculated Ti isotopic ratios in the He shell of TP-AGB stars. The results are given in Table 3. Different cases correspond to different values of the mean neutron exposure (and thus of the initial metallicity of the star). All the Ti isotopes, especially ^{50}Ti , are enhanced with respect to ^{48}Ti . These results do not differ much from our previous predictions for the nucleosynthesis in the He shell that were used for comparison of the SiC data by Ireland, Zinner, & Amari (1991a, b) and Amari et al. (1991b). The most significant difference concerns the value of $\delta^{50}\text{Ti}$, that has increased because of the strong reduction of the ^{50}Ti cross section at low temperature. As already noticed by Ireland et al. (1991a) and by Hoppe et al. (1993), the Ti anomalies produced by the s -process in the He shell alone cannot account for the large spread of the measured data.

By adopting the model of mixing He-processed matter from the He shell to the envelope described in § 2, we can estimate the Ti surface composition in stars of different mass and metal

content. However, as in the case of Si, the initial Ti composition of the envelopes in which SiC grains condensed can only be inferred if the galactic chemical evolution of the Ti isotopes is known.

Most of the solar Ti ($\sim 74\%$) is in the form of ^{48}Ti . Consequently, the spectroscopic observation of a Ti enhancement relative to Fe in stars of metallicity lower than the solar one, similar to the Si enhancement, indicates that ^{48}Ti is most likely enhanced. But this does not exclude that, as in the case of ^{29}Si and ^{30}Si , other Ti isotopes can be enhanced too: it depends on whether they can be largely produced in massive stars. Present theoretical predictions for the yields of both Types Ia and II SNe are not as constraining as in the case of Si, since they underestimate the contributions to the solar abundances of all Ti isotopes.

On the other hand, we saw that the meteoritic data show a linear correlation of $\delta^{46}\text{Ti}$ with $\delta^{29}\text{Si}$ and $\delta^{30}\text{Si}$, whose slope is ~ 1 . This suggests that in the stellar envelopes where SiC condensed, the small enhancement of ^{46}Ti with respect to ^{48}Ti had the same origin as that of $^{29,30}\text{Si}$ with respect to ^{28}Si . As a consequence, we would expect an enhancement of ^{46}Ti with respect to ^{48}Ti at metallicities lower than the solar one. Since the spectroscopic observations of Ti give $[\text{Ti}/\text{Fe}] \approx +0.3$ in the halo and this is expected to be essentially ^{48}Ti , we may infer that $[\text{Ti}/\text{Fe}] = +0.5$ dex in the halo.

Hence, from the analysis of Ti anomalies in interstellar SiC grains, we deduce that $\sim 70\%$ of ^{48}Ti and all the ^{46}Ti are produced in Type II SNe in a primary way. As in the case of the Si isotopes, detailed calculations of Ti isotope yields in stellar models of different metallicities are needed.

Figures 4–6 display the results of our models in the Ti three-isotope plot when also an enhancement $[\text{Ti}/\text{Fe}] = +0.4$ is assumed in the halo, with a corresponding linear decrease for disk stars according to the simplified law $[\text{Ti}/\text{Fe}] = -0.4$ [Fe/H]. As for ^{50}Ti , the results shown in the figures have been obtained under the hypothesis that its abundance scales with that of iron during galactic evolution. The predicted corre-

TABLE 3
Ti ISOTOPE COMPOSITIONS IN THE HE SHELL OF TP-AGB STARS

ISOTOPE	[Fe/H], τ_0 (mbarn $^{-1}$)						
	−0.52, 0.277	−0.35, 0.215	−0.22, 0.179	−0.12, 0.154	−0.05, 0.137	+0.00, 0.128	+0.10, 0.109
Production Factors ($X_i^{\text{fin}}/X_i^{\text{ini}}$)							
^{46}Ti	2.864	2.738	2.631	2.537	2.453	2.403	2.275
^{47}Ti	1.304	1.172	1.082	1.015	0.962	0.932	0.867
^{48}Ti	0.557	0.534	0.520	0.512	0.507	0.505	0.515
^{49}Ti	4.794	4.418	4.242	4.159	4.123	4.114	3.957
^{50}Ti	33.67	23.24	17.93	14.72	12.57	11.49	9.421
δ -Values ($\delta^i\text{Ti}$)							
^{46}Ti	4.14 (3)	4.13 (3)	4.06 (3)	3.96 (3)	3.84 (3)	3.76 (3)	3.42 (2)
^{47}Ti	1.34 (3)	1.19 (3)	1.08 (3)	0.82 (2)	0.97 (2)	0.86 (2)	0.83 (2)
^{49}Ti	7.61 (3)	7.27 (3)	7.16 (3)	7.12 (3)	7.13 (3)	7.15 (3)	6.68 (3)
^{50}Ti	5.94 (4)	4.25 (4)	3.35 (4)	2.78 (4)	2.38 (4)	2.18 (4)	1.73 (4)
Initial Compositions (X_i^{ini})							
^{46}Ti	1.22 (−7)	1.51 (−7)	1.73 (−7)	1.93 (−7)	2.13 (−7)	2.23 (−7)	2.49 (−7)
^{47}Ti	1.01 (−7)	1.29 (−7)	1.52 (−7)	1.75 (−7)	1.96 (−7)	2.08 (−7)	2.36 (−7)
^{48}Ti	9.21 (−7)	1.23 (−6)	1.49 (−6)	1.76 (−6)	2.02 (−6)	2.15 (−6)	2.50 (−6)
^{49}Ti	7.89 (−8)	1.02 (−7)	1.20 (−7)	1.37 (−7)	1.55 (−7)	1.64 (−7)	1.86 (−7)
^{50}Ti	1.48 (−8)	3.33 (−8)	5.92 (−8)	9.38 (−8)	1.31 (−7)	1.64 (−7)	2.59 (−7)

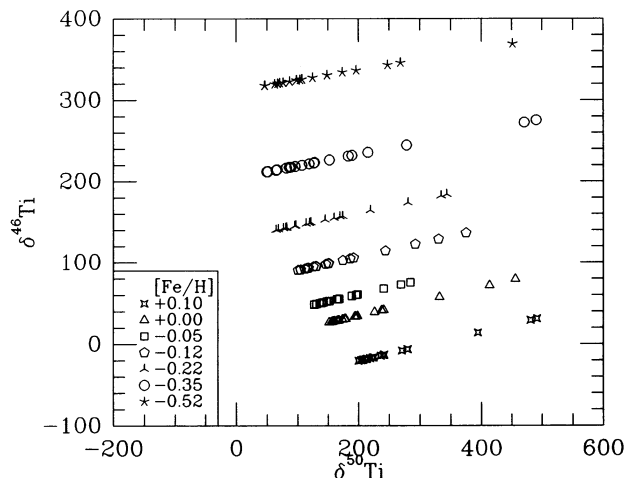


FIG. 4.—Three-isotope plot $\delta^{46}\text{Ti}$ vs. $\delta^{50}\text{Ti}$, showing the results of our calculations in TP-AGB stars. Each sequence of data corresponds to stellar models of given metallicity and initial mass ranging from 1.5 to 1.7 M_{\odot} .

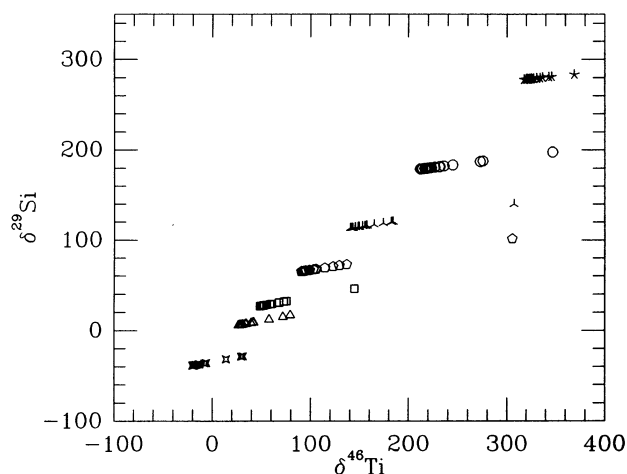


FIG. 7.—The predicted correlation between $\delta^{29}\text{Si}$ and $\delta^{46}\text{Ti}$ in TP-AGB stars of 1.5–1.7 M_{\odot} and different metallicities.

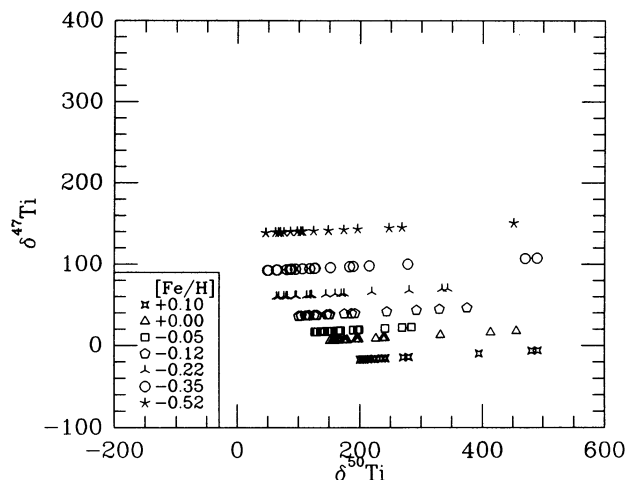


FIG. 5.—As in Fig. 4, but for $\delta^{47}\text{Ti}$ vs. $\delta^{50}\text{Ti}$

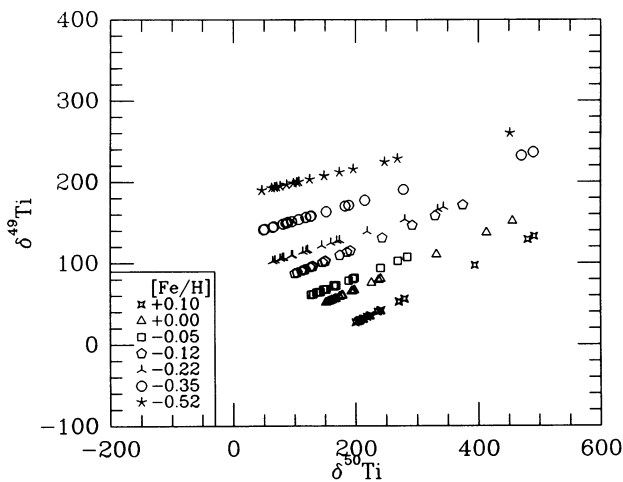


FIG. 6.—As in Fig. 4, but for $\delta^{49}\text{Ti}$ vs. $\delta^{50}\text{Ti}$

lations between $\delta^{29}\text{Si}$ and $\delta^i\text{Ti}$ are shown in Figures 7–9. In the case of $\delta^{29}\text{Si}$ versus $\delta^{47}\text{Ti}$, the main correlation produced by changing the metallicity has nearly the same slope as for $\delta^{29}\text{Si}$ versus $\delta^{49}\text{Ti}$, but the spread due to the *s*-process is much lower, since ^{47}Ti has a higher neutron capture cross section than ^{49}Ti . All ^iTi excesses and correlations in SiC grains appear fairly consistent with our predictions; only the calculated $\delta^{50}\text{Ti}$ seems a bit too high. Indeed, the very small neutron capture cross section of the neutron magic nucleus ^{50}Ti makes it behave as a bottleneck in the *s*-path, building up a considerable abundance. It is worthwhile to notice that the SiC grains do actually show a large spread of $\delta^{50}\text{Ti}$, that is an evident signature of *s*-processing. A possible overall displacement of $\delta^{50}\text{Ti}$ toward lower values to better match the SiC data could be obtained with a less drastic departure of the ^{50}Ti neutron capture cross section from the $1/v$ law.

5.1. Titanium Anomalies from Massive Stars?

In order to estimate the Ti isotope compositions in massive stars in the layers where $\text{C/O} \sim 1$ we took the data from the calculations of Raiteri et al. (1993). The neutron exposure when

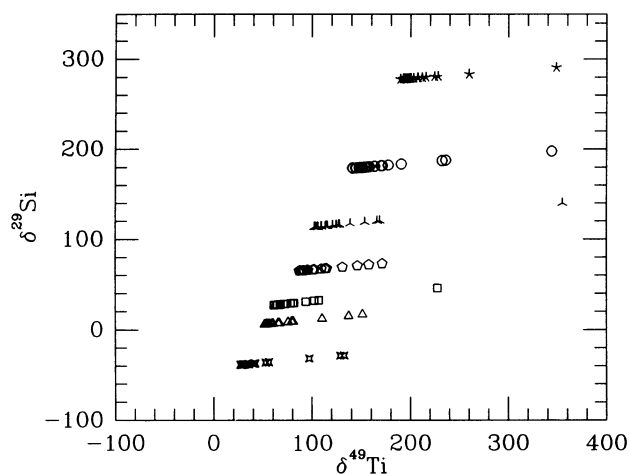
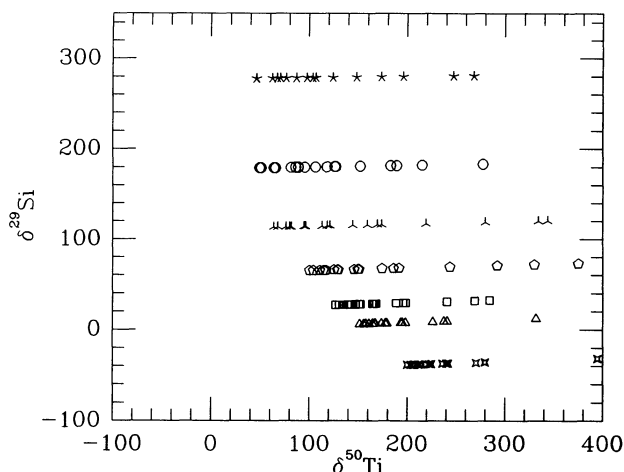
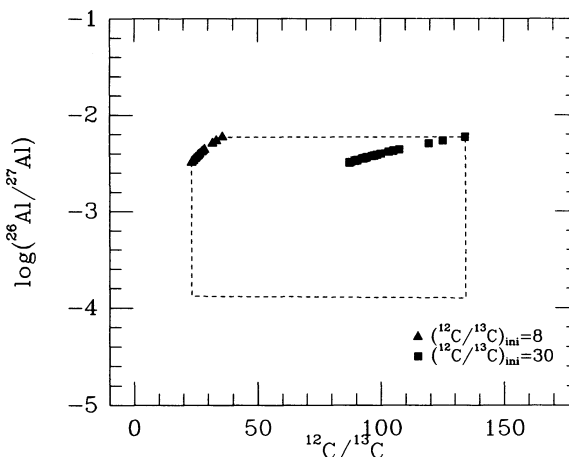


FIG. 8.—As in Fig. 7, but for $\delta^{29}\text{Si}$ vs. $\delta^{49}\text{Ti}$

FIG. 9.—As in Fig. 7, but for $\delta^{29}\text{Si}$ vs. $\delta^{50}\text{Ti}$ FIG. 10.—The $^{26}\text{Al}/^{27}\text{Al}$ ratio in the envelope of solar metallicity stars of $1.5\text{--}1.7 M_{\odot}$ just before leaving the AGB. Two cases are shown, where the initial $^{12}\text{C}/^{13}\text{C}$ ratio on the AGB is 8 (triangles) or 30 (squares). The dashed area indicates the range of $^{26}\text{Al}/^{27}\text{Al}$ values that can be predicted since the beginning of the TP-AGB phase.

the above requirement is met during He burning is low: $\tau = 0.0123 \text{ mbarn}^{-1}$, and $\delta^{46}\text{Ti} = 626$, $\delta^{47}\text{Ti} = -57$, $\delta^{49}\text{Ti} = 7122$, and $\delta^{50}\text{Ti} = 1967$. These results are at odd with the measurements in SiC even when considering a possible dilution with material carrying solar Ti abundances, and strengthen the conclusion that massive stars are unlikely sources of SiC grains.

6. ALUMINUM ANOMALY

In a recent paper Forestini, Paulus, & Arnould (1991) examined the production of ^{26}Al in low-mass AGB stars. They found that in the H shell of a $3 M_{\odot}$ star, at the typical temperature of $40\text{--}50 \times 10^6 \text{ K}$, proton captures on ^{25}Mg transform about all the initial ^{25}Mg into ^{26}Al , without the need to invoke the operation of the so-called Mg-Al cycle. Consequently, in a star of solar metallicity the H-processed zone would contain an ^{26}Al abundance by mass of 6×10^{-5} .

We followed the above prescription in order to calculate the $^{26}\text{Al}/^{27}\text{Al}$ ratio in the H shell of our TP-AGB stellar models, using, however, a different procedure for mixing the dredge-up material with the stellar envelope. In fact, the ashes of the H shell are gradually engulfed by the next thermal pulse, where ^{26}Al is destroyed by neutron captures when the ^{13}C source is activated; the residual amount of ^{26}Al present in the upper He zone will be later ingested by the growing thermal instability, experiencing the second minor neutron burst by the ^{22}Ne source. At the end of the pulse, the ^{26}Al mass fraction in the partially He consumed zone is $\sim 10^{-5}$. Hence, each third dredge-up episode mixes $\sim 10^{-8} M_{\odot}$ of ^{26}Al with the surface.

Figure 10 shows the resulting $(^{26}\text{Al}/^{27}\text{Al})$ in the stellar envelope of TP-AGB stars at the last pulse (filled symbols) as a function of the $^{12}\text{C}/^{13}\text{C}$ ratio for 20 stellar models of 1.5 to $1.7 M_{\odot}$. The dashed area indicates the range of $^{26}\text{Al}/^{27}\text{Al}$ values that can be predicted since the beginning of the TP-AGB phase. As for the initial $^{12}\text{C}/^{13}\text{C}$ ratio, two extreme cases are considered in the range of spectroscopic observation of M stars: in one case (indicated by triangles) the initial ratio on the AGB is assumed to be 8, in the second one (indicated by squares) 30. A change in the initial metal content of the star does not affect these results, unless a different evolution of ^{27}Al and ^{25}Mg as a function of $[\text{Fe}/\text{H}]$ were recognized.

Refractory aluminum is much more abundant in SiC than magnesium, probably condensed as AlN in solid solution or as

subgrains (Hoppe et al. 1994; Anders & Zinner 1993) at similar reducing conditions as SiC. The comparison between the predicted values with the meteoritic data shows that the above picture can explain the higher $^{26}\text{Al}/^{27}\text{Al}$ in single SiC grains (leaving the X grains aside).

However, it is not easy to give account of the large spread of measured values, and of the fact that only half SiC show extinct ^{26}Al . As discussed in Hoppe et al. (1994), a contamination of meteoritic samples with Al from extraneous sources, apparently carried by oxide grains (Amari et al. 1991), cannot be ruled out, so that the real $^{26}\text{Al}/^{27}\text{Al}$ ratio in many SiC grains could be higher. A second comment concerns the ^{26}Al decay in the stellar envelope, before SiC grains condense. As a matter of fact, the half-life of ^{26}Al is $6 \times 10^5 \text{ yr}$, and a certain decrease of the $^{26}\text{Al}/^{27}\text{Al}$ ratio in SiC grains with respect to the above predictions is possible. The expected ^{26}Al yield from TP-AGB stars needs a deeper analysis, but the demanding problem is the experimental determination of the rate of the reaction $^{26}\text{Al}(n, p)^{26}\text{Mg}$, the most efficient channel to consume ^{26}Al in s-process conditions. For it, only theoretical estimates are available (Caughlan & Flower 1988).

7. CARBON AND NITROGEN ISOTOPE ANOMALIES

7.1. Carbon Anomaly

The spectroscopic $^{12}\text{C}/^{13}\text{C}$ ratio in red giants having suffered the first dredge-up has been determined by several authors; in particular, Gilroy (1989) analyzed red giants in ~ 20 galactic open clusters and correlated this ratio with the stellar mass. She found that $^{12}\text{C}/^{13}\text{C}$ increases linearly with stellar mass from 1 to $2 M_{\odot}$, going from ~ 8 to 30 , and then levels off. Since the standard theory of stellar evolution can account only for a narrower range of values around the observed upper limit (Iben 1977), it is necessary to postulate that for many carbon stars a kind of extramixing of H-processed matter with the envelope had occurred before the TP-AGB phase. We have adopted initial $^{12}\text{C}/^{13}\text{C}$ ratios of 8 and 30 to span the observational range. The continuous increase of $^{12}\text{C}/^{13}\text{C}$ in the envelope by the addition of ^{12}C -rich matter dredge-up from the He shell then easily explains the spread of $^{12}\text{C}/^{13}\text{C}$ observed in carbon stars (Smith & Lambert

1990), matching the carbon isotope anomalies in the majority of SiC grains.

There are, however, two minor populations of SiC grains, called A and B, detected in Murchison (Amari et al. 1991b), highly enriched in ^{13}C , with $^{12}\text{C}/^{13}\text{C}$ from ≤ 2 to 3.5, and between 3.5 and ~ 10 , respectively. A few grains with similar characteristics have been also observed in other chondrites (Stone et al. 1991a; Alexander 1993). These groups likely find their observational counterpart in carbon stars of type J (Lambert et al. 1986) that are not discussed here.

Concerning the possible effect of a differential galactic evolution of C isotopes, its examination would require a better understanding of the uncertain origin of cosmic ^{13}C .

7.2. Nitrogen Anomaly

A huge spread of nitrogen anomaly is also apparent in single SiC grains. The $^{14}\text{N}/^{15}\text{N}$ ratio ranges from less than solar (272) to $\sim 10^4$. The standard stellar evolutionary theory predicts that the first dredge-up, while decreasing the ^{12}C abundance by about one-third, roughly doubles that of ^{14}N (Iben 1977), and decreases ^{15}N by 30%–50% (Dearborn, Tinsley, & Schramm 1978; El Eid 1993).

As a consequence, one would expect that in red giant stars the $^{14}\text{N}/^{15}\text{N}$ ratio be ≤ 1000 . But since the occurrence of an extramixing is claimed for explaining the whole range of carbon composition in the spectra of red giants that have not yet reached the TP-AGB phase, the same process would also affect nitrogen isotopes, with a resulting spread of the $^{14}\text{N}/^{15}\text{N}$ ratio up to much higher values. Moreover, the $^{14}\text{N}/^{15}\text{N}$ ratio in the envelope may be further slightly modified by the effect of the third dredge-up. As a matter of fact, this latter carries to the surface material both from the He and from the H shell: in the H shell an enhanced ^{14}N and a lower amount of ^{15}N results from the CN cycling, while in the subsequent He shell ^{14}N is completely destroyed by α -captures.

A few observations of carbon stars and circumstellar envelopes (Kahane et al. 1988; see discussion in Gustafsson 1989 and Omont 1993) yield $^{14}\text{N}/^{15}\text{N}$ ratios that exceed 3000. Wannier et al. (1991) inferred the $^{14}\text{N}/^{15}\text{N}$ abundance ratio in eight carbon stars, including two proton-planetary nebulae. In all cases (but one) they found lower limits that are significantly larger than the terrestrial ratio, going up to 4400. The only exception is Y CVn, a ^{13}C -rich star with $^{14}\text{N}/^{15}\text{N} > 70$, that is actually a J-type star. A smaller $^{14}\text{N}/^{15}\text{N}$ ratio in this kind of objects appears to be in agreement with the values measured in SiC grains of populations A and B.

We do not intend to pursue the analysis any further, but just notice that a contamination of SiC samples with normal nitrogen cannot be completely excluded.

An open problem remains the galactic evolution of the $^{14}\text{N}/^{15}\text{N}$ ratio, and the specific cases of SiC grains of the mainstream population showing a slight heavy nitrogen enrichment.

8. CONCLUSIONS

In this paper a possible interpretation of the silicon and titanium isotope anomalies measured in meteoritic SiC grains has been advanced in terms of stellar *s*-nucleosynthesis in TP-AGB stars of low mass and of the galactic evolution of Si and Ti isotopes.

We found that the Si anomalies can be explained by assuming that in the envelopes of carbon stars, where the grains form, a small *s*-process signature carried by He-shell matter mixed with the envelope superposed to the original, slightly nonsolar isotope Si composition. Such anomalous compositions in stars of metallicities close to solar are inferred by assuming that the galactic abundances of ^{29}Si and ^{30}Si are entirely due to a mostly primary nucleosynthesis in Type II SNe, together with $\sim 70\%$ of ^{28}Si , whereas the remaining $\sim 30\%$ derives from the delayed production of Type Ia SNe.

This hypothesis is not in contradiction with the present knowledge of stellar nucleosynthesis and must be tested through improved calculations of nucleosynthesis in stellar models of different metallicity. A detailed analysis of the chemical evolution of the Galaxy and of possible local inhomogeneities is also required.

The above approach has then been employed to explain the Ti anomalies in the same grains. We found that these are satisfactorily accounted for if, in addition to ^{48}Ti , also ^{46}Ti , ^{47}Ti , and ^{49}Ti are considered to be primary species, being enhanced with respect to iron in stars of lower than solar metallicity. As in the case of Si, refined stellar modeling is needed to ascertain the reliability of our assumptions.

The analysis of both Si and Ti anomalies favors a multiple star origin of SiC grains, with stars of slightly different metal content (within 0.2 dex the solar one) contributing to the production of the measured SiC grains. Grains from more metal poor stars were presumably ejected in the interstellar medium earlier in the average and destroyed before being trapped inside of carbonaceous chondrites.

The presence of extinct ^{26}Al in SiC grains has been examined. When coupling the nucleosynthesis occurring in the H shell and in the He shell of TP-AGB stars, we obtained $^{26}\text{Al}/^{27}\text{Al}$ ratios in the envelope that essentially agree with the bulk of the measured data.

Further indications in favor of a multiple star origin for the SiC grains comes from the analysis of the C and N anomalies. In particular, the $^{12}\text{C}/^{13}\text{C}$ ratio observed in different optical carbon stars ranges between 20 and ≈ 100 , in agreement with the observed spread of data.

The interpretation suggested in this paper does not pretend to explain all the problems connected with the Si, Ti, and Mg anomalies in SiC grains: in particular, SiC grains belonging to minor populations, such as the *X* and the *Z* ones, require further investigation. The same holds for the populations A and B showing low $^{12}\text{C}/^{13}\text{C}$. The most plausible explanation for these latter grains is that they come from giant stars that are observed to be carbon-rich, but are not enriched in *s*-elements: the J-type carbon stars.

We are indebted to C. M. O'D. Alexander, E. Anders, M. Arnould, H. Beer, A. Chieffi, M. W. Howard, F. Käppeler, D. L. Lambert, M. Limongi, C. Sharp, O. Straniero, F. X. Timmes, G. J. Wasserburg, and in particular to D. D. Clayton and S. E. Woosley for helpful discussions. We want to deeply thank E. Zinner, S. Amari, and P. Hoppe from the Washington University, and R. S. Lewis from the University of Chicago, for continuous exchanges of data and ideas. We are grateful to F.-K. Thielemann for suggestions and advice.

REFERENCES

- Alexander, C. M. O'D. 1993, *Geochim. Cosmochim. Acta*, 57, 2869
- Amari, S., Hoppe, P., Zinner, E., & Lewis, R. 1992, *ApJ*, 394, L43
- Amari, S., Zinner, E., & Lewis, R. 1991a, *Lunar Planet. Sci.*, XXII, 19
- . 1991b, *Meteoritics*, 26, 314
- Anders, E., & Zinner, E. 1993, *Meteoritics*, 28, 490
- Bao, Z. Y., & Käppeler, F. 1987, *Atomic Data Nucl. Data*, 36, 411
- Beer, H. 1992, private communication
- Beer, H., Voss, F., & Winters, R. R. 1992, *ApJS*, 80, 403
- Bernatowicz, T. J., Amari, S., & Lewis, R. S. 1992, *Lunar Planet. Sci.*, XXIII, 91
- Bernatowicz, T. J., Amari, S., Zinner, E., & Lewis, R. S. 1991, *ApJ*, 373, L73
- Branch, D., Doggett, J. B., Nomoto, K., & Thielemann, F.-K. 1985, *ApJ*, 294, 619
- Brown, L. E., & Clayton, D. D. 1992, *ApJ*, 392, L79
- . 1993, in *Nuclei in the Cosmos*, ed. F. Käppeler & K. Wisshak (Bristol: Institute of Physics), 525
- Busso, M., Chieffi, A., Gallino, R., Limongi, M., Raiteri, C. M., & Straniero, O. 1993, in *IAU Symp. 155, Planetary Nebulae*, ed. R. Weinberger & A. Acker (Dordrecht: Kluwer), 361
- Busso, M., Gallino, R., Lambert, D. L., Raiteri, C. M., & Smith, V. V. 1992, *ApJ*, 399, 218
- Busso, M., Lambert, D. L., Beglio, L., Gallino, R., Raiteri, C. M., & Smith, V. V. 1994, in preparation
- Caughlan, G. R., & Fowler, W. A. 1988, *Atomic Data Nucl. Data*, 40, 283
- Chan, S. J., & Kwok, S. 1990, *A&A*, 237, 354
- Chieffi, A., Limongi, M., & Straniero, O. 1993, private communication
- Clayton, D. D. 1977, *Earth Planet. Sci. Lett.*, 35, 398
- . 1988, *ApJ*, 334, 191
- Dearborn, D., Tinsley, B. M., & Schramm, D. N. 1978, *ApJ*, 223, 557
- El Eid, M. 1993, in *Proc. 7th Workshop on Nuclear Astrophysics*, ed. W. Hillebrandt & M. Müller (München: MPA), 149
- Edvardsson, B., Andersen, J., Gustafsson, B., Lambert, D. L., Nissen, P. E., & Tomkin, J. 1993, *A&A*, 275, 101
- Forestini, M., Paulus, G., & Arnould, M. 1991, *A&A*, 252, 597
- Gallino, R., Busso, M., Picchio, G., & Raiteri, C. M. 1990, *Nature*, 348, 298
- Gallino, R., Raiteri, C. M., & Busso, M. 1992, *Ann. Geophys. Suppl.*, 10, C465
- . 1993, *ApJ*, 410, 400
- Gilroy, K. K. 1989, *ApJ*, 347, 835
- Gustafsson, B. 1989, *ARA&A*, 27, 701
- Hashimoto, M., Nomoto, K., Tsujimoto, T., & Thielemann, F.-K. 1993, in *Nuclei in the Cosmos*, ed. F. Käppeler & K. Wisshak (Bristol: Institute of Physics), 587
- Hoppe, P., Amari, S., Zinner, E., Ireland, T. R., & Lewis, R. S. 1994, *ApJ*, 430, 870
- Hoppe, P., Geiss, J., Bühler, F., Neuenschwander, J., Amari, S., & Lewis, R. S. 1993a, *Geochim. Cosmochim. Acta*, 57, 4059
- Hoppe, P., Sterbel, R., Eberhardt, P., Amari, S., & Lewis, R. S. 1993b, *Meteoritics*, 28, 363
- Huss, G. R., Deloule, E., Hutcheon, I. D., & Wasserburg, G. J. 1993, *Meteoritics*, 28, 368
- Huss, G. R., Hutcheon, I. D., & Wasserburg, G. J. 1993, *Lunar Planet. Sci.*, XXIV, 687
- Iben, I., Jr. 1977, in *Advanced Stages in Stellar Evolution*, ed. P. Bouvier & A. Maeder (Sauverny: Geneva Obs.), 1
- Iben, I., Jr., & Renzini, A. 1984, *Phys. Rep.*, 105, 329
- Ireland, T. R., Zinner, E., & Amari, S. 1991a, *ApJ*, 376, L53
- . 1991b, *Lunar Planet. Sci.*, XXII, 613
- Kahane, C., Gomez-Gonzales, J., Cernicharo, J., & Guelin, M. 1988, *A&A*, 190, 167
- Käppeler, F., Gallino, R., Busso, M., Picchio, G., & Raiteri, C. M. 1990, *ApJ*, 354, 630
- Khokhlov, A. M. 1991, *A&A*, 245, L25
- Lambert, D. L. 1989, in *Cosmic Abundances of Matter*, ed. C. J. Waddington (New York: AIP), 168
- Lambert, D. L., Gustafsson, B., Eriksson, K., & Hinkle, K. H. 1986, *ApJS*, 62, 373
- Larimer, J. W., & Bartholomay, M. 1979, *Geochim. Cosmochim. Acta*, 43, 1455
- Lattimer, J. M., Schramm, D. N., & Grossman, L. 1978, *ApJ*, 219, 230
- Lee, T., Papanastassiou, D. A., & Wasserburg, G. J. 1977, *ApJ*, 211, L107
- Lewis, R. S., Amari, S., & Anders, E. 1990, *Nature*, 348, 293
- . 1994, *Geochim. Cosmochim. Acta*, 58, 471
- Lodders, K., & Fegley, B., Jr. 1993, *Earth Planet. Sci. Lett.*, 117, 125
- Maline, G., Hartmann, D. H., Clayton, D. D., & Mathews, G. J. 1993, *ApJ*, 413, 633
- Matteucci, F., & François, P. 1989, *MNRAS*, 239, 885
- Matteucci, F., & Greggio, L. 1986, *A&A*, 154, 279
- Nomoto, K., Shigeyama, T., Yanagita, S., Hayakawa, S., & Yasuda, K. 1990, in *Chemical and Dynamical Evolution of Galaxies*, ed. F. Ferrini, J. Franco, & F. Matteucci (Pisa: ETS), 366
- Obradovic, M., Brown, L. E., Guha, S., & Clayton, D. D. 1991, *Meteoritics*, 26, 381
- Omont, A. 1993, in *Nuclei in the Cosmos*, ed. F. Käppeler & K. Wisshak (Bristol: Institute of Physics), 65
- Ott, U., & Begemann, F. 1990, *ApJ*, 353, L57
- Ott, U., Begemann, F., Yang, J., & Epstein, S. 1988, *Nature*, 332, 700
- Prantzos, N., Doom, C., Arnould, M., & de Loore, C. 1986, *ApJ*, 304, 695
- Prombo, C. A., Podosek, F. A., Amari, S., & Lewis, R. S. 1993, *ApJ*, 410, 393
- Raiteri, C. M., Gallino, R., Busso, M., Neuberger, D., & Käppeler, F. 1993, *ApJ*, 419, 207
- Ryan, S. G., Norris, J. E., & Bessell, M. S. 1991, *AJ*, 102, 303
- Sackmann, I.-J., & Boothroyd, A. I. 1991a, in *IAU Symp. 145, Evolution of Stars: The Photospheric Abundance Connection*, ed. G. Michaud & A. Tutukov (Dordrecht: Kluwer), 375
- Sackmann, I.-J., & Boothroyd, A. I. 1991b, *ApJ*, 366, 529
- Smith, V. V., & Lambert, D. L. 1990, *ApJS*, 72, 387
- Shigeyama, T., Nomoto, K., Yamaoka, H., & Thielemann, F.-K. 1992, *ApJ*, 386, L13
- Stone, J., Hutcheon, I. D., Epstein, S., & Wasserburg, G. J. 1991a, in *Stable Isotope Geochemistry: A Tribute to Samuel Epstein*, ed. H. P. Taylor, Jr., J. R. O'Neil, & I. R. Kaplan (Columbus, OH: Geochemical Soc.), 487
- . 1991b, *Earth Planet. Sci. Lett.*, 107, 570
- Tang, M., & Anders, E. 1988, *Geochim. Cosmochim. Acta*, 52, 1235
- Tang, M., Anders, E., Hoppe, P., & Zinner, E. 1989, *Nature*, 339, 351
- Thielemann, F.-K., & Arnett, W. D. 1985, *ApJ*, 295, 604
- Thielemann, F.-K., Hashimoto, M., & Nomoto, K. 1990, *ApJ*, 349, 222
- Thielemann, F.-K., Nomoto, K., & Yokoi, Y. 1986, *A&A*, 158, 17
- Timmes, F. X., Woosley, S. E., & Weaver, T. A. 1993, in *Proc. 6th Advanced School of Astrophysics (São Paulo)*, ed. B. Barbuy, J. A. Freites Pacheco, & E. Janot Pacheco (São Paulo: IAGUSP), 333
- Virag, A., Wopenka, B., Amari, S., Zinner, E., Anders, E., & Lewis, R. S. 1992, *Geochim. Cosmochim. Acta*, 56, 1715
- Vassiliadis, E., & Wood, P. R. 1993, *ApJ*, 413, 641
- Wagemans, C., D'hondt, P., & Brissot, R. 1993, in *Nuclei in the Cosmos*, ed. F. Käppeler & K. Wisshak (Bristol: Institute of Physics), 247
- Wannier, P. G., Andersson, B.-G., Olofsson, H., Ukita, N., & Young, K. 1991, *ApJ*, 380, 593
- Wasserburg, G. J. 1985, in *Protostars and Planets II*, ed. D. C. Black & G. S. Matthews (Tucson: Univ. of Arizona Press), 703
- Wasserburg, G. J., Busso, M., Gallino, R., & Raiteri, C. M. 1994, *ApJ*, 424, 412
- Weaver, T. A., & Woosley, S. E. 1993, *Phys. Rep.*, 227, 65
- Williams, P. M., van der Hucht, K. A., Bouchet, P., Spoelstra, T. A. Th., Eenens, P. R. J., Geballe, T. R., Kidger, M. R., & Churchwell, E. 1992, *MNRAS*, 258, 461
- Woosley, S. E. 1986, in *Nucleosynthesis and Chemical Evolution*, ed. B. Hauck, A. Maeder, & G. Meynet (Sauverny: Geneva Obs.), 1
- Woosley, S. E., & Weaver, T. A. 1980, *ApJ*, 238, 1017
- . 1982, in *Essays in Nuclear Astrophysics*, ed. C. A. Barnes, D. D. Clayton, & D. N. Schramm (Cambridge Univ. Press), 237
- Zinner, E., Amari, S., Anders, E., & Lewis, R. S. 1991a, *Nature*, 349, 51
- Zinner, E., Amari, S., & Lewis, R. S. 1991b, *ApJ*, 382, L47
- Zinner, E., Tang, M., & Anders, E. 1987, *Nature*, 330, 730
- . 1989, *Geochim. Cosmochim. Acta*, 53, 3273